Comparative analysis of electron-gas excitations on a spherical surface and on a flat plane

1996 J. Phys.: Condens. Matter 8 10241

(http://iopscience.iop.org/0953-8984/8/49/015)

J. Phys.: Condens. Matter **8** (1996) 10241–10252. Printed in the UK

Comparative analysis of electron-gas excitations on a spherical surface and on a flat plane

Takeshi Inaoka

Department of Materials Science and Technology, Faculty of Engineering, Iwate University, 4-3-5 Ueda, Morioka, Iwate 020, Japan

Received 9 May 1996, in final form 18 September 1996

Abstract. By using the random-phase approximation and the f-sum rule approach, we make a comparative analysis of multipole excitation modes in an electron gas confined on a spherical surface (SSEG) and normal modes in an electron gas constrained to a flat plane (i.e. a two-dimensional electron gas (2DEG)). In the SSEG, we investigate the size dependence of multipole modes by varying the electron number and the sphere radius a simultaneously with the average electron density fixed. The L/a dependence of multipole-mode energies, where L denotes the multipole order, is compared with the energy dispersion of normal modes in the 2DEG. The series of the highest-energy multipole modes corresponds to the two-dimensional (2D) plasmon branch, while all the other multipole modes correspond to the single-particle excitation (SPE) continuum. With decrease in L/a, each multipole mode acquires more definite character of collective excitation or SPE, and the highest-energy multipole mode starts to occupy the greater part of the f-sum intensity. As L increases with L/a fixed, the components of the highest-energy multipole mode and all the other multipole modes in the f-sum intensity approach those of the 2D plasmon mode and the SPE modes at the corresponding wavenumber in the f-sum intensity, respectively. This indicates that multipole modes with higher L are more analogous in character to normal modes in the 2DEG. This analysis elucidates similarities and differences between multipole modes in the SSEG and normal modes in the 2DEG.

1. Introduction

Recent development of synthetic techniques has made it possible to produce a variety of materials with layered electron systems. Quasi-two-dimensional (2D) electron systems can be formed at semiconductor–insulator interfaces such as Si–SiO_2 [1–3] and at semiconductor heterojunctions such as GaAs/$Al_xGa_{1-x}As$ [4–7]. The monolayer graphite on transition-metal carbide surfaces also exhibits 2D character in its electronic properties [8, 9]. In a family of fullerene molecules, the electron systems are localized around spherical hollow-cage structures of carbon atoms [10, 11]. In a species of carbon nanotubes, some of which are metallic, the electron systems are localized around cylindrical tube structures of carbon atoms [12]. We can understand the essential features of excitations in these layered electron systems by examining the dynamical response of those electron gases which are confined on flat planes [13–17], spherical surfaces [18] and cylindrical surfaces [19–21]. This simplified description of layered electron systems allows us to perform most of our calculations analytically, although we have to beware of its limitations in representing real systems.

Our previous work has investigated the size dependence of multipole excitation modes in an electron gas confined on a spherical surface [18]. Hereafter, this electron gas will be

0953-8984/96/4910241+12$19.50

abbreviated as SSEG. In this work, the radius of the sphere is varied with the mean electron density fixed, and the dynamical response of the SSEG is treated within the random-phase approximation (RPA). A multipole mode higher than a dipole mode is composed of various electronic transition processes involving change in the orbital angular momentum l. The above investigation has shown that, with increase in the size, each multipole mode acquires a more definite character of collective excitation or single-particle excitation (SPE). This gradual variation in the mode character, which stems from the finiteness of the SSEG, can be analysed quantitatively by evaluating the contribution of each constituent transition process to the energy-loss intensity of the mode.

In the present work, we make a comparative analysis of multipole modes in the SSEG and normal modes in an electron gas constrained to a flat plane (i.e. a two-dimensional electron gas (2DEG)). The SSEG resembles the 2DEG in that these electron systems are both sharply localized in one direction, namely in the radial or plane-normal direction. On the other hand, the SSEG differs from the 2DEG in that the former is finite. In multipole modes of the SSEG, the arc length $2\pi a/L$, where a and L signify the sphere radius and the multipole order, respectively, characterizes the variation in the induced charge density along the spherical surface, and L/a corresponds to the wavenumber Q in the 2DEG. The L/a dependence of multipole-mode energies is compared with the energy dispersion of normal modes in the 2DEG. The mode character is reflected in the energy-loss intensity of the mode. As a multipole mode takes a more collective excitation character, it occupies a greater fraction of the f sum of the energy-loss intensity. On the other hand, as a multipole mode acquires a more SPE character, it occupies a smaller fraction of the f-sum intensity. With a change in the multipole order L, we examine the f-sum intensity and its distribution among multipole modes at chosen L/a, in comparison with the f-sum intensity and its distribution among normal modes at the corresponding wavenumber Q. This comparative analysis reveals similarities and differences between multipole modes in the SSEG and normal modes in the 2DEG.

2. Theory

In this section, we represent an essential part of a theoretical scheme for the following analysis. Details of the theoretical scheme for multipole modes in the SSEG have already been given in [18]. By means of the RPA, we investigate the dynamical response of an electron system to the external potential U oscillating in time with angular frequency ω.

First, we formulate the multipole response of the SSEG. For simplicity of treatment, we assume that the SSEG is spherically symmetric in its ground state, namely that a finite number of electrons with a closed-shell configuration are confined by a one-electron potential of spherical symmetry. Each energy eigenstate is specified by l and m, namely the orbital angular momentum and the magnetic quantum numbers, and its angular dependence is described by a spherical harmonic $Y_{lm}(\theta, \phi)$ in spherical polar coordinates with their origin at the centre of the sphere. Eigenstates of $l > 0$ are degenerate with respect to m, and a group of $2(2l+1)$-fold degenerate states including spin constitute an electron shell, which is labelled l. Each occupied electron shell is completely filled in a closed-shell configuration. The energy of an electron shell l is expressed as

$$\epsilon_l = \hbar^2 l(l+1)/2\mu a^2 \tag{1}$$

with the electron mass μ and the sphere radius a. The energy ϵ_l represents the centrifugal potential energy or, in other words, the kinetic energy along the spherical surface. The (L, M) component $U_{LM}(\omega)Y_{LM}(\theta, \phi)$ of the external potential at the spherical surface

gives rise to the same component $\delta\sigma_{LM}(\omega)Y_{LM}(\theta,\phi)$ of the induced areal charge density and, consequently, the component $V_{LM}(\omega)Y_{LM}(\theta,\phi)$ of the total potential at the spherical surface. The total potential V is composed of the external potential U and the induced Coulomb potential generated by $\delta\sigma$. The (L, M) components $\delta\sigma_{LM}(\omega)$ and $V_{LM}(\omega)$ can be determined by the following equations:

$$\delta\sigma_{LM}(\omega) = \chi_L^0(\omega)V_{LM}(\omega) \tag{2}$$

$$V_{LM}(\omega) = U_{LM}(\omega) + \frac{4\pi a}{2L+1}\delta\sigma_{LM}(\omega) \tag{3}$$

where the susceptibility $\chi_L^0(\omega)$ takes the form

$$\chi_L^0(\omega) = \frac{e^2}{2\pi a^2}\sum_{l,l'}(2l+1)(2l'+1)\begin{pmatrix} l & l' & L \\ 0 & 0 & 0 \end{pmatrix}^2 \frac{f(\epsilon_l)-f(\epsilon_{l'})}{\epsilon_l-\epsilon_{l'}+\hbar\omega+\mathrm{i}\eta}. \tag{4}$$

In this equation, $f(\epsilon)$ and η denote the Fermi–Dirac distribution function for eigenstates and an infinitesimal positive constant, respectively, and the spin degeneracy is taken into account. The parenthesized (2×3) array of numbers signifies the Wigner $3j$ symbol, whose value vanishes unless $|l'-l| \leqslant L \leqslant l+l'$ and $l+l'+L =$ even integer [22]. The $3j$ symbol prescribes which electronic transition processes contribute to excitations of the electron system. The dielectric function is given by

$$\epsilon_L(\omega) = U_{LM}(\omega)/V_{LM}(\omega) = 1 - \frac{4\pi a}{2L+1}\chi_L^0(\omega). \tag{5}$$

The energy-loss function defined by

$$F_L(\omega) = \mathrm{Im}\left[-1/\epsilon_L(\omega)\right] \tag{6}$$

describes the intensity of the energy loss which occurs in response to the (L, M) component of U. In equation (6), the symbol Im denotes the imaginary part. Energy values of excitation modes are given by the zeros of $\epsilon_L(\omega)$, and the integrated energy-loss intensity I of each mode is defined by the area of the corresponding resonance peak in the ω dependence of $F_L(\omega)$:

$$I = \int_{peak} F_L(\omega)\ \mathrm{d}(\hbar\omega) = \int_{peak}\mathrm{Im}\left[-1/\epsilon_L(\omega)\right]\ \mathrm{d}(\hbar\omega). \tag{7}$$

The dielectric function defined in equation (5) as the ratio of $U_{LM}(\omega)$ to $V_{LM}(\omega)$ does not depend upon M and, consequently, the energy and the energy-loss intensity of each excitation mode are independent of M, when M is varied in the allowed range $-L \leqslant M \leqslant L$ with L fixed.

As seen from equations (2) and (3), each transition process occurs in response to the total potential V involving contributions of all the transition processes. This indicates that each transition process interacts with itself spuriously. We require the self-interation correction (SIC) to examine quantitatively the electronic structure [23, 24] and excitation [25, 26] of small systems such as small metal spheres [23, 25, 26] and spherical metal shells [24]. In small metal clusters with electron number $N \leqslant 40$, the SIC yields an appreciable red shift of the surface-plasmon energy, which leads to better agreement with experimental results (see table 2 in [25] or [26]). In our analysis, we calculate multipole modes in the SSEG in a broad size region $8 \leqslant N \leqslant 1352$. Although our treatment without the SIC may cause appreciable inaccuracy in the smallest N range in this broad size region, it has no substantial influence on our analysis in the next section.

The dynamical response of the 2DEG can be formulated in a similar manner to that of the SSEG [13]. Each excitation mode specified by wavevector $\boldsymbol{Q}$ and angular frequency ω is described by the following pair of equations:

$$\delta\sigma(\boldsymbol{Q},\,\omega) = \chi^0(\boldsymbol{Q},\,\omega)V(\boldsymbol{Q},\,\omega) \tag{8}$$

$$V(\boldsymbol{Q},\,\omega) \;= U(\boldsymbol{Q},\,\omega) + (2\pi/Q)\;\delta\sigma(\boldsymbol{Q},\,\omega) \tag{9}$$

where the susceptibility $\chi^0(\boldsymbol{Q},\,\omega)$ is written in the form

$$\chi^0(\boldsymbol{Q},\,\omega) = 2e^2\int\frac{\mathrm{d}^2\boldsymbol{K}}{(2\pi)^2}\,\frac{f(\boldsymbol{K}+\boldsymbol{Q}) - f(\boldsymbol{K})}{\epsilon(\boldsymbol{K}+\boldsymbol{Q}) - \epsilon(\boldsymbol{K}) + \hbar\omega + \mathrm{i}\eta}. \tag{10}$$

In this equation, $\epsilon(\boldsymbol{K})$ is the energy dispersion of electrons given by $\epsilon(\boldsymbol{K}) = \hbar^2\boldsymbol{K}^2/2\mu$, and $f(\boldsymbol{K})$ is the Fermi–Dirac distribution function for electron state $\boldsymbol{K}$. The dielectric function $\epsilon(\boldsymbol{Q},\,\omega)$ is given by

$$\epsilon(\boldsymbol{Q},\,\omega) = U(\boldsymbol{Q},\,\omega)/V(\boldsymbol{Q},\,\omega) = 1 - (2\pi/Q)\chi^0(\boldsymbol{Q},\,\omega) \tag{11}$$

and the energy-loss function $F(\boldsymbol{Q},\,\omega)$ is defined by

$$F(\boldsymbol{Q},\,\omega) = \mathrm{Im}[-1/\epsilon(\boldsymbol{Q},\,\omega)]. \tag{12}$$

For each 2D plasmon mode, the integrated energy-loss intensity I is defined by

$$I = \int_{peak} F(\boldsymbol{Q},\,\omega)\;\mathrm{d}(\hbar\omega) = \int_{peak}\mathrm{Im}[-1/\epsilon(\boldsymbol{Q},\,\omega)]\;\mathrm{d}(\hbar\omega) \tag{13}$$

in the same manner as in equation (7). At temperature $T = 0$, the Fermi–Dirac distribution function $f(\boldsymbol{K})$ becomes a step function, and the $\boldsymbol{K}$ integral in equation (10) can be performed analytically [13].

Next, we derive the f-sum rules, namely the sum rules for the energy-loss function of the SSEG and the 2DEG. The susceptibility $\chi_L^0(\omega)$ in equation (2) or $\chi^0(\boldsymbol{Q},\,\omega)$ in equation (8) describes the independent-particle response to the total self-consistent potential V. Alternatively, we can introduce the susceptibility χ that describes the response of interacting electrons to the external potential U. In terms of χ, we can generally express the induced charge density $\delta\rho$ in real space as

$$\delta\rho(\boldsymbol{r},\,\omega) = \int\mathrm{d}^3\boldsymbol{r}'\;\chi(\boldsymbol{r},\,\boldsymbol{r}',\,\omega)U(\boldsymbol{r}',\,\omega). \tag{14}$$

The susceptibility $\chi(\boldsymbol{r},\,\boldsymbol{r}',\,\omega)$ is what is called the retarded density correlation function. The susceptibility $\chi(\boldsymbol{r},\,\boldsymbol{r}',\,\omega)$ satisfies the following sum rule [27]:

$$\frac{1}{\pi}\int_{-\infty}^{\infty}\mathrm{d}\omega\;\omega\;\mathrm{Im}[\chi(\boldsymbol{r},\,\boldsymbol{r}',\,\omega)] = \frac{e^2}{\mu}\big[n_0(\boldsymbol{r})\;\Delta\delta(\boldsymbol{r}-\boldsymbol{r}') + \boldsymbol{\nabla}n_0(\boldsymbol{r})\cdot\boldsymbol{\nabla}\delta(\boldsymbol{r}-\boldsymbol{r}')\big] \tag{15}$$

where $n_0(\boldsymbol{r})$ is the number density of interacting electrons in the ground state, and Δ and $\boldsymbol{\nabla}$ signify the Laplacian and the gradient operator, respectively, with respect to $\boldsymbol{r}$. We apply the general sum rule in equation (15) to our special cases of the SSEG and the 2DEG. The SSEG can be regarded as an electron system sharply localized around a spherical surface at $r = a$, and the ground-state density $n_0(\boldsymbol{r})$ is assumed to be spherically symmetric. The susceptibility $\chi_L(\omega)$ describing the $(L,\,M)$ excitation mode as

$$\delta\sigma_{LM}(\omega) = \chi_L(\omega)U_{LM}(\omega) \tag{16}$$

can be obtained by integrating $\chi(\boldsymbol{r},\,\boldsymbol{r}',\,\omega)$ as

$$\chi_L(\omega) = \frac{1}{a^2}\int\mathrm{d}^3\boldsymbol{r}\int\mathrm{d}^3\boldsymbol{r}'\;Y_{LM}^*(\theta,\,\phi)\chi(\boldsymbol{r},\,\boldsymbol{r}',\,\omega)Y_{LM}(\theta',\,\phi') \tag{17}$$

and the Dirac δ function in equation (15) can be written as

$$\delta(\boldsymbol{r}-\boldsymbol{r}') = \frac{\delta(r-r')}{r^2}\sum_{L,M} Y_{LM}(\theta,\,\phi)Y^*_{LM}(\theta',\,\phi') \tag{18}$$

in terms of spherical harmonics. The two variable sets of $(r,\,\theta,\,\phi)$ and $(r',\,\theta',\,\phi')$ are the spherical polar coordinates that represent the position vectors $\boldsymbol{r}$ and $\boldsymbol{r}'$, respectively. By using equations (17) and (18), we can convert the general expression (15) to the sum rule for $\chi_L(\omega)$:

$$\frac{1}{\pi}\int_{-\infty}^{\infty} \mathrm{d}\omega\;\omega\;\mathrm{Im}\big[\chi_L(\omega)\big] = -L(L+1)\frac{n_s e^2}{\mu a^2} \tag{19}$$

where n_s is the electron number per unit area in the ground state. The dielectric function $\epsilon_L(\omega)$ is related to $\chi_L(\omega)$ by

$$\frac{1}{\epsilon_L(\omega)} = 1 + \frac{4\pi a}{2L+1}\chi_L(\omega) \tag{20}$$

and the real and imaginary parts of $\epsilon_L(\omega)$ are an even function and an odd function, respectively, of ω. Accordingly, equation (19) can be rewritten as

$$R_{tl} \equiv \int_0^{\infty} \mathrm{d}\omega\;\omega\;\mathrm{Im}\left[-\frac{1}{\epsilon_L(\omega)}\right] = \frac{\pi}{2}\frac{L(L+1)}{2L+1}\frac{4\pi n_s e^2}{\mu a}. \tag{21}$$

This is the f-sum rule for multipole excitations in the SSEG.

The 2DEG is an electron system sharply localized around a plane, and the ground-state density $n_0(\boldsymbol{r})$ is assumed to be uniform along the plane. The susceptibility $\chi(\boldsymbol{Q},\,\omega)$ describing the $\boldsymbol{Q}$ mode as

$$\delta\sigma(\boldsymbol{Q},\,\omega) = \chi(\boldsymbol{Q},\,\omega)U(\boldsymbol{Q},\,\omega) \tag{22}$$

is given by

$$\chi(\boldsymbol{Q},\,\omega) = \frac{1}{A}\int \mathrm{d}^3\boldsymbol{r}\int \mathrm{d}^3\boldsymbol{r}'\;\exp(-\mathrm{i}\boldsymbol{Q}\cdot\boldsymbol{R})\chi(\boldsymbol{r},\,\boldsymbol{r}',\,\omega)\;\exp(\mathrm{i}\boldsymbol{Q}\cdot\boldsymbol{R}') \tag{23}$$

where A is the area of the plane and $\boldsymbol{R}$ represents the plane-parallel component of $\boldsymbol{r}$. For the δ function in equation (15), we employ the expression

$$\delta(\boldsymbol{r}-\boldsymbol{r}') = \delta(z-z')\frac{1}{A}\sum_{Q}\exp[\mathrm{i}\boldsymbol{Q}\cdot(\boldsymbol{R}-\boldsymbol{R}')] \tag{24}$$

where the z axis is taken to be normal to the plane. With the aid of equations (23) and (24), we can obtain the sum rule for $\chi(\boldsymbol{Q},\,\omega)$:

$$\frac{1}{\pi}\int_{-\infty}^{\infty}\mathrm{d}\omega\;\omega\;\mathrm{Im}[\chi(\boldsymbol{Q},\,\omega)] = -\frac{n_s e^2}{\mu}\boldsymbol{Q}^2 \tag{25}$$

which leads to the f-sum rule already known [13]:

$$R_{tl} \equiv \int_0^{\infty}\mathrm{d}\omega\;\omega\;\mathrm{Im}\left[-\frac{1}{\epsilon(\boldsymbol{Q},\,\omega)}\right] = \frac{\pi}{2}\frac{2\pi n_s e^2}{\mu}Q. \tag{26}$$

3. Analysis

By means of the theoretical framework in the preceding section, we examine multipole excitation modes in the SSEG in an order range $1 \leqslant L \leqslant 5$ and normal modes in the 2DEG. In the SSEG, we vary the electron number N and the sphere radius a simultaneously with the average electron density n_s fixed, and we choose electron systems with closed-shell configurations. The fixed n_s-value corresponds to the electron density parameter $r_s = 2$, where r_s is related to n_s by

$$\pi\left(r_s a_B\right)^2 n_s = 1 \tag{27}$$

with the Bohr radius $a_B = \hbar^2/\mu e^2$. The sphere radius a can be expressed as

$$a/a_B = \sqrt{N} r_s/2 \tag{28}$$

in terms of N and r_s. We employ the same n_s-value for the 2DEG also. We can compare the size dependence of multipole-mode energies of the SSEG in figure 1(a) with the energy dispersion of normal modes of the 2DEG in figure 1(b). In the SSEG, the electron number N is varied in the range $8 \leqslant N \leqslant 1352$. The arc length $\lambda_L = 2\pi a/L$ in the SSEG characterizes the variation in the induced charge density along the spherical surface in a similar fashion to the wavelength $\lambda = 2\pi/Q$ in the 2DEG. Accordingly, the value of L/a in the SSEG can be considered to correspond to the wavenumber Q in the 2DEG. In figure 1(a), full circles, full triangles, open circles, open triangles and open squares indicate energy values of multipole modes of order $L = 1$, 2, 3, 4 and 5, respectively, as functions of L/a. In figure 1(b), a curve and a shaded area represent the dispersion branch of 2D plasmons and the SPE continuum, respectively. Plasmon modes decay away when they enter the SPE continuum. The abscissa and the ordinate are both indicated on a logarithmic scale and in atomic units (au). In figure 1(a), the broken and chain lines are the guide lines of $(L/a)^{1/2}$ and L/a, respectively, to view the size dependence. Similarly, in figure 1(b), the broken and chain lines are the guide lines of $Q^{1/2}$ and Q, respectively, to see the Q dependence. As exhibited in figure 1(a), energy values of the highest-energy multipole modes in the SSEG line up substantially on the same curve independent of L, which corresponds to the plasmon branch of the 2DEG in figure 1(b). On the other hand, the energy values of all the other multipole modes in the SSEG are dispersed in a lower region, and the upper series of the energy points corresponds to the upper edge of the SPE continuum in figure 1(b). With decrease in L/a and Q, the sequence of the highest-energy multipole modes and the plasmon branch begin to vary as $(L/a)^{1/2}$ and $Q^{1/2}$, respectively, while the upper series of the lower multipole modes and the upper edge of the SPE continuum start to vary as L/a and Q, respectively. Figure 2 displays only the energy points of $L = 5$ extracted from figure 1(a). The L/a dependence of mode energies in each order of $1 \leqslant L \leqslant 4$ can be deduced from figure 1 in our previous work [18], although the plot in this figure is for a narrower size range $8 \leqslant N \leqslant 512$. A dipole mode of $L = 1$ is constituted only by the transition process from l_F to $l_F + 1$ ($\Delta l = 1$). Here, l_F denotes the angular momentum of the highest occupied shell. A quadrupole mode of $L = 2$ is made up of two transition processes of $l_F \to l_F + 2$ and $l_F - 1 \to l_F + 1$ ($\Delta l = 2$) unless $l_F = 0$. A multipole mode of higher L is composed of a larger number of transition processes involving a change in l.

We focus our attention on multipole modes of $L = 5$ in figure 2. When $l_F \leqslant 4$, that is $L/a \leqslant \sqrt{2}/r_s$ au, each mode is composed of five transition processes of $\Delta l = 5$ ($l_F \to l_F + 5,\ l_F - 1 \to l_F + 4,\ l_F - 2 \to l_F + 3,\ l_F - 3 \to l_F + 2,\ l_F - 4 \to l_F + 1$), three processes of $\Delta l = 3$ ($l_F \to l_F + 3,\ l_F - 1 \to l_F + 2,\ l_F - 2 \to l_F + 1$) and one process of $\Delta l = 1$ ($l_F \to l_F + 1$). These nine processes in all lead to nine modes at each size, except

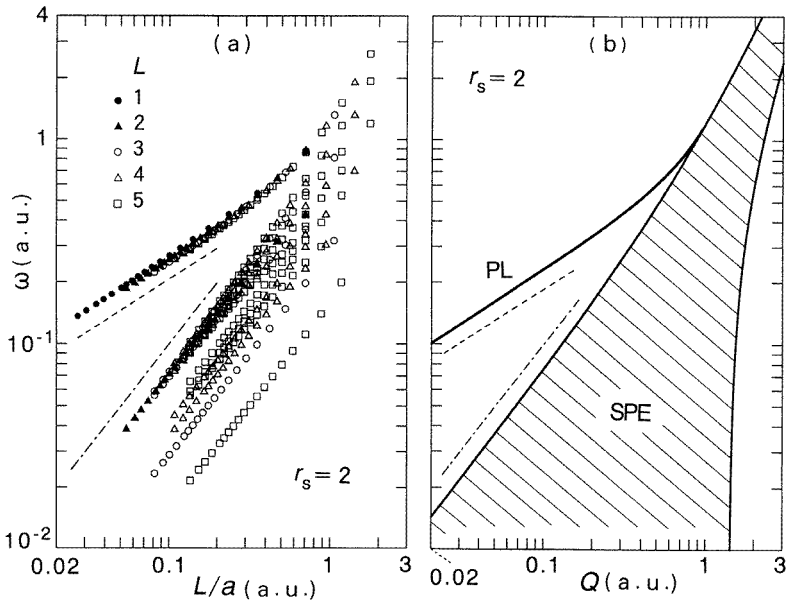

Figure 1. Comparison of (a) the L/a dependence of multipole-mode energies in the SSEG with (b) the energy dispersion of normal modes in the 2DEG. The fixed average electron density corresponds to the electron density parameter $r_s = 2$. In (b), PL and SPE denote the plasmon branch and the single-particle excitation continuum, respectively.

for the case of $l_F = 4$ where two of these processes happen to have the same energy change. We let $\omega(l \to l')$ denote the energy change involved in the process of $l \to l'$. With decrease in L/a, the values of $\omega(l \to l')$ for $\Delta l = 5$ or 3 gradually converge to form a fine series that is separate from other $\omega(l \to l')$ values in energy distribution and that varies as a^{-1}. A transition process operates to enhance the energy-loss intensity when its energy change $\omega(l \to l')$ is lower than the mode energy, while a transition process acts to reduce the energy-loss intensity when its energy change $\omega(l \to l')$ is higher than the mode energy. At each size, the energy of the highest-energy mode is higher than any value of $\omega(l \to l')$ and, in this mode, all the constituent transition processes cooperate to enhance the energy-loss intensity. With decrease in L/a, the energy of the highest-energy mode begins to become definitely separated from the energy values of other modes, and the constituent transition processes tend to make more comparable contributions to the excitation. This indicates that the highest-energy mode acquires a more collective excitation character [18]. Next, we turn our attention to lower-energy modes. Each energy of these modes intervenes between two adjacent values of $\omega(l \to l')$. Accordingly, following the above-mentioned size dependence of $\omega(l \to l')$, with decrease in L/a, energy values of these modes start to vary as a^{-1} and divide into two fine series and one isolated value, as exhibited in figure 2. As L/a becomes smaller, a small number of transition processes whose energy changes are close to the mode energy start to make the dominant contribution to the energy-loss intensity, and there occurs a stronger cancellation between those transition processes whose energy changes are just below and above the mode energy. This implies that lower-energy modes take more SPE character with decrease in L/a [18]. Incidentally, when the mode energy lies between two series of $\omega(l \to l')$ with different l changes, this variation in the mode character is not so

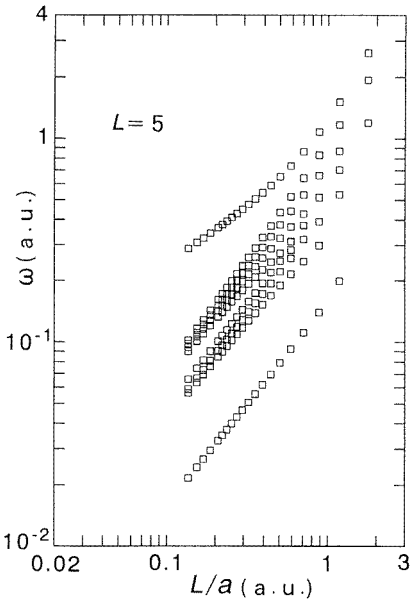

Figure 2. L/a dependence of multipole-mode energies with $L = 5$, drawn from the entire plot in figure 1(a).

remarkable as it is when the mode energy is caught in one series of $\omega(l \rightarrow l')$. In the 2DEG, as shown in the energy dispersion diagram in figure 1(b), excitation modes divide distinctly into collective excitations and SPE, namely the 2D plasmon branch and the SPE continuum. In the SSEG, however, with decrease in L/a, multipole modes gradually gain more definite character of collective excitation or SPE. This gradual evolution of the mode character originates from the finiteness of the SSEG.

Figure 3(a) displays the integrated resonance intensity I of each multipole mode at $L/a = \sqrt{2}/4$ au. The position of each bar represents the energy of each multipole mode on the abscissa, and the symbol on each bar tip shows the resonance intensity I of each mode on the ordinate. Various kinds of symbol designate multipole orders in the same manner as in figure 1(a). Figure 3(b) exhibits the ω dependence of the energy-loss function $F(Q, \omega)$ in the SPE continuum and the integrated resonance intensity I of the 2D plasmon mode at $Q = \sqrt{2}/4$ au. In each part of figure 3, the abscissa and the ordinate are both indicated on a logarithmic scale. In each multipole order L (>1), the highest-energy mode has a much stronger resonance intensity I than any other mode, and its I value is close to that of the 2D plasmon mode. This analysis of the energy-loss intensity confirms the above observation that the highest-energy multipole mode corresponds to the 2D plasmon mode, while other multipole modes correspond to the SPE continuum. Figure 4 exhibits the values of R_{tl} and $R_{tl} - R_{hm}$ for multipole modes at $L/a = \sqrt{2}/4$ au and for normal modes at $Q = \sqrt{2}/4$ au. The multipole order L is indicated on the abscissa together with the assignment to the 2DEG. The arrows point to the scale (either on the left- or the right-hand side) which is relevant to a series of points connected by broken lines. As already defined in equations (21) and (26), the total intensity R_{tl} represents the f sum of the energy-loss intensity that is obtained by integrating ω Im$[-1/\epsilon_L(\omega)]$ or ω Im$[-1/\epsilon(Q, \omega)]$ over the whole positive range of ω. In the SSEG, this intensity involves one, two, four, six and nine

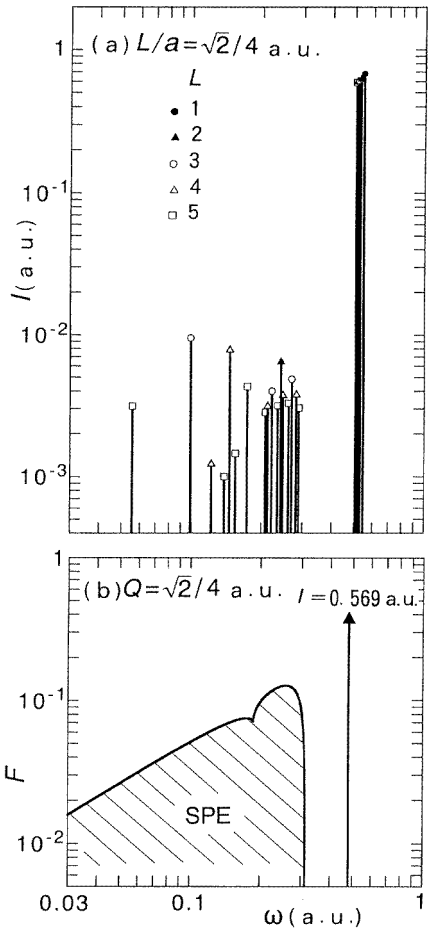

Figure 3. Energy-loss intensity of (a) multipole modes at $L/a = \sqrt{2}/4$ au in the SSEG and (b) normal modes at $Q = \sqrt{2}/4$ au in the 2DEG. In (a), the integrated energy-loss intensity I of each multipole mode is indicated by a vertical bar at the corresponding value of ω. The symbol on each bar tip represents the multiple order L. In (b), the value of the energy-loss function F is shown as a function of ω for the SPE modes, and the integrated energy-loss intensity I of the 2D plasmon mode is indicated by a vertical arrow at the corresponding value of ω with its intensity value.

multipole modes for $L = 1$, 2, 3, 4 and 5, respectively, and in the 2DEG, it includes both a 2D plasmon mode and the SPE continuum. The symbol R_{hm} indicates the component of the highest-energy mode in the f-sum intensity. Accordingly, the value of $R_{tl} - R_{hm}$ is equal to the sum of the resonance intensity over all the multipole modes but the highest-energy mode in the SSEG or over the SPE continuum in the 2DEG. Although not shown in figure 4, the value of $R_{tl} - R_{hm}$ vanishes at $L = 1$, because there is only one mode. As seen from the difference between the ordinate scale on the left- and right-hand sides, the values of $R_{tl} - R_{hm}$ are two orders of magnitude smaller than those of R_{tl}. This implies that, in the same way as the plasmon mode in the 2DEG, the highest-energy mode in the SSEG occupies the greater part of the total resonance intensity R_{tl}, because of its growing

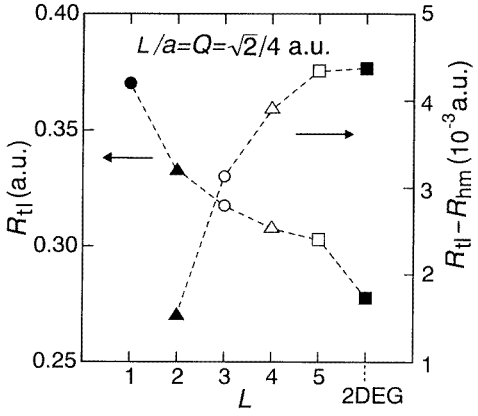

Figure 4. f-sum rule analysis of multipole modes at $L/a = \sqrt{2}/4$ au in the SSEG and normal modes at $Q = \sqrt{2}/4$ au in the 2DEG. The symbol R_{tl} on the left-hand side denotes the f-sum intensity of the energy-loss function, while the symbol R_{hm} on the right-hand side represents the component of the highest-energy mode in the f-sum intensity. The multipole order L is indicated on the abscissa together with the assignment to the 2DEG.

collective excitation character. With increase in L, the value of R_{tl} decreases toward that of the 2DEG, and the value of $R_{tl} - R_{hm}$ increases towards that of the 2DEG. Since L/a and Q have the same value, the ratio of the R_{tl}-value of the SSEG to that of the 2DEG is given by $(L + 1)/(L + 1/2)$ from equations (21) and (26). Accordingly, as L becomes larger, the value of R_{tl} of the SSEG approaches that of the 2DEG comparatively slowly. The above L dependence of R_{tl} and $R_{tl} - R_{hm}$ suggests that multipole modes with higher L in the SSEG are similar in character to normal modes in the 2DEG. A multipole mode with higher L consists of a larger number of transition processes, and it possesses a more definite character of collective excitation or SPE.

As in other small particles, multipole modes in the SSEG should adequately be observed by electron energy-loss spectroscopy combined with scanning transmission electron microscopy [28, 29]. This combined technique can observe multipole modes of individual particles or SSEGs by means of a highly focused electron beam of several ångströms width that can be scanned around target systems. We can control multipole orders of excited modes by varying the impact parameter and the incident energy that is typically in the range 50–100 keV. The results of these measurements can be analysed by treating an incident electron as a classical charged particle moving along a straight line and by calculating the dynamical response of the target system to the external potential generated by the passing electron [29–32]. Each (L, M) component $U_{LM}(\omega)$ of the external potential at the spherical surface can be obtained by expanding the external potential $U(\boldsymbol{r}, t)$ in terms of spherical harmonics $Y_{LM}(\theta, \phi)$ and by Fourier transforming it with respect to time. Following the theoretical framework in section 2, we can calculate the dynamical response of the SSEG to each (L, M) component $U_{LM}(\omega)$.

4. Summary

By using the RPA and the f-sum rule approach, we have made a comparative analysis of multipole excitation modes in a SSEG and normal modes in a 2DEG. In the SSEG, the electron number and the sphere radius a are varied simultaneously with the average

electron density fixed. The quantity L/a in the SSEG, where L denotes the multipole order, corresponds to wavenumber Q in the 2DEG. A multipole mode with higher L is composed of a larger number of transition processes involving angular momentum change. The results are summarized as follows:

(1) When we compare the L/a dependence of multipole-mode energies with the energy dispersion of normal modes in the 2DEG, we notice that the series of the highest-energy multipole modes corresponds to the 2D plasmon branch, while other multipole modes correspond to the SPE continuum. The latter multipole modes form not a continuous but a discrete energy distribution because of the finiteness of the SSEG. With increase in L, a larger number of multipole modes are dispersed in a lower-energy region corresponding to the SPE continuum of the 2DEG.

(2) With decrease in L/a, the highest-energy multipole mode starts to become distinctly separated in energy from other modes and takes a more collective excitation character. On the other hand, as L/a becomes smaller, other multipole modes gradually create an organized energy distribution owing to various angular momentum changes involved in constituent transition processes and acquire more SPE character. This gradual evolution of the mode character originates from the finiteness of the SSEG.

(3) The highest-energy multipole mode occupies the greater part of the f sum of the energy-loss intensity owing to its growing collective excitation character, when it becomes well separated in energy from other lower modes. With increase in L, the components of the highest-energy multipole mode and all the other modes in the f-sum intensity approach those of the 2D plasmon mode and the lower SPE modes at the corresponding wavenumber in the f-sum intensity, respectively. This implies that multipole modes with higher L bear a stronger resemblance in character to normal modes in the 2DEG.

Acknowledgments

The author expresses his thanks to A Tamura for a stimulating discussion which motivated the present work. He is also grateful to H Ojima for her assistance in preparing the manuscript and figures. Numerical calculations in this work were performed at the Iwate University Computer Centre.

References

[1] Fowler A B, Fang F F, Howard W E and Stiles P J 1966 *Phys. Rev. Lett.* **16** 901
[2] Ando T, Fowler A B and Stern F 1982 *Rev. Mod. Phys.* **54** 437, and references therein
[3] Nicollian E H and Brews J R 1982 *MOS Physics and Technology* (New York: Wiley), and references therein
[4] Dingle R, Störmer H L, Gossard A C and Wiegmann W 1978 *Appl. Phys. Lett.* **33** 665
[5] Störmer H L, Dingle R, Gossard A C, Wiegmann W and Sturge M D 1979 *Solid State Commun.* **29** 705
[6] Hiyamizu S, Mimura T, Fujii T and Nanbu K 1980 *Appl. Phys. Lett.* **37** 805
[7] Hiyamizu S, Mimura T, Fujii T, Nanbu K and Hashimoto H 1981 *Japan. J. Appl. Phys.* **20** L245
[8] Nagashima A, Nuka K, Itoh H, Ichinokawa T, Oshima C, Otani S and Ishizawa Y 1992 *Solid State Commun.* **83** 581
[9] Nagashima A, Nuka K, Satoh K, Itoh H, Ichinokawa T, Oshima C and Otani S 1993 *Surf. Sci.* **287–288** 609
[10] Kroto H W, Heath J R, O'Brien S C, Curl R F and Smalley R E 1985 *Nature* **318** 162
[11] Kikuchi K, Nakahara N, Wakabayashi T, Suzuki S, Shiromaru H, Miyake Y, Saito K, Ikemoto I, Kainosho M and Achiba Y 1992 *Nature* **357** 142
[12] Iijima S 1991 *Nature* **354** 56
[13] Stern F 1967 *Phys. Rev. Lett.* **18** 546
[14] Das Sarma S and Quinn J J 1982 *Phys. Rev.* B **25** 7603
[15] Jain J K and Allen P B 1985 *Phys. Rev.* B **32** 997

[16] Tzoar N and Zhang C 1986 *Phys. Rev.* B **34** 1050
[17] Peeters F M, Wu Xiaoguang and Devreese J T 1987 *Phys. Rev.* B **36** 7518
[18] Inaoka T 1992 *Surf. Sci.* **273** 191
[19] Sato O, Tanaka Y, Kobayashi M and Hasegawa A 1993 *Phys. Rev.* B **48** 1947
[20] Sato O, Tanaka Y, Kobayashi M and Hasegawa A 1994 *J. Phys. Soc. Japan* **63** 4186
[21] Yannouleas C, Bogachek E N and Landman U 1994 *Phys. Rev.* B **50** 7977
[22] See, e.g. Messiah A 1961–2 *Quantum Mechanics* (Amsterdam: North-Holland) appendix C
[23] Ishii Y, Ohnishi S and Sugano S 1986 *Phys. Rev.* B **33** 5271
[24] Inaoka T 1995 *J. Phys. Soc. Japan* **64** 1658
[25] Saito S, Bertsch G F and Tománek D 1991 *Phys. Rev.* B **43** 6804
[26] Pacheco J M and Ekardt W 1992 *Ann. Phys. (Lpz.)* **1** 254
[27] Griffin A and Harris J 1976 *Can. J. Phys.* **54** 1396
[28] Batson P E 1982 *Phys. Rev. Lett.* **49** 936
[29] Ugarte D, Colliex C and Trebbia P 1992 *Phys. Rev.* B **45** 4332
[30] Schmeits M 1981 *J. Phys. C: Solid State Phys.* **14** 1203
[31] Das P C and Gersten J I 1983 *Phys. Rev.* B **27** 5412
[32] Ferrell T L and Echenique P M 1985 *Phys. Rev. Lett.* **55** 1526